A novel OFDM-CPM modulation scheme and its application in WDM-PON

Yufeng Shao (邵宇丰), Junwen Zhang (张俊文), Wuliang Fang (方武良), Shumin Zou (邹书敏), Xinying Li (李欣颖), Bo Huang (黄 博), Nan Chi (迟 楠)*, and Siyuan Yu (余思远)

Department of Communication Science and Engineering, and State Key Lab of ASIC & System, Fudan University, Shanghai 200433, China

**E-mail: nanchi@fudan.edu.cn*

Received June 2, 2010

A novel scheme to generate, transmit, and receive an optical orthogonal frequency division multiplexing (OFDM) continuous phase modulation (CPM) signal, which is combining minimum shift keying (MSK) coding with OFDM optical modulation, for downlink application in a 4×2.5-Gb/s wavelength division multiplexing (WDM) passive optical access network, is proposed and experimentally validated. We also realize wavelength remodulation for carrying upstream on-off keying (OOK) data to reduce the cost budget at the optical network unit. The experimental results show that the power penalties for the downlink and the uplink data after transmission over 25-km SMF-28 fiber are 0.1 dB and smaller than 0.4 dB, respectively.

OCIS codes: 060.2330, 060.2360, 060.4080.
doi: 10.3788/COL20100809.0894.

Optical orthogonal frequency division multiplexing (OOFDM) has been shown to be effective in mitigating the influence of chromatic dispersion and polarization mode dispersion (PMD) for high capacity single wavelength fiber links[1−3]. Recently, a few reported OOFDM access passive optical network (PON) solutions with the use of wavelength division multiplexing (WDM) technology, can be used to support various applications, achieve high spectral efficiency, and realize the flexibility to dynamically allocate the bandwidth among the optical network units (ONUs). It is a promising approach to meet the requirements of future access networks[4−6]. Generally, an optical OFDM signal is generated by multi-level quadrature amplitude modulation (MQAM) or multi-level phase shift keying (MPSK) coding and is selected as a downstream signal or a upstream signal[7−12], which could cause discontinuous phase transition between the adjacent symbols. As a result, the digital signal processing (DSP) equipment at the receiver is more complex and unstable. It is well known that minimum shift keying (MSK) is a special form of continuous phase modulation (CPM)[13], with the property of fast decaying side-lobe. When MSK is employed as the coder for OFDM, this property can mitigate the effect of phase noise and carrier frequency offset (CFO), and thus reduces the inter-carrier interference (ICI) caused by many reasons.

In this letter, the detailed operational principles of optical OFDM-CPM generation and detection are presented. Based on our experiment, we compare the optical spectrum property of OFDM-CPM, OFDM-2PSK, and OFDM-QPSK. The performance analysis of OFDM-CPM downlink signal in a 4×2.5-Gb/s WDM access PON system is experimentally introduced, and the bit-error ratio (BER) performance of OFDM-CPM is measured to outperform that of OFDM-QPSK on the downstream channel. The experimental results prove that the OFDM-CPM signal generated and used as downlink signal is suitable for simultaneously offering higher receiver performance and simplifying DSP for the future optical access network.

As we know, MSK is the simplest form of a CPM signal and can be expressed as[14]

$$y_{\rm MSK}(t)=\sqrt{\frac{2E_{\rm b}}{T_{\rm b}}}\cos\left\{2\pi\left[f_{\rm c}+\frac{1}{T_{\rm b}}\left(\frac{1}{4}+\frac{u_k-1}{2}\right)\right]t+\theta_k\right\},kT_{\rm b}\le t\le(k+1)T_{\rm b},\tag{1}$$

where $E_{\rm b}$ is the pulse energy per transmitted bit, $T_{\rm b}$ is one bit period, $f_{\rm c}$ is the center carrier frequency, $u_k=0$ or 1 is the binary data being transmitted at a rate of $R=1/T_{\rm b}$, and θ_k is a phase constant which is valid over the kth binary data interval $kT_{\rm b}\le t\le(k+1)T_{\rm b}$. As shown in Eq. (1), the signal frequency change takes place at higher frequency for data "1" and lower frequency for data "0". Depending on the input binary data, the phase of signal changes: data "1" increase the phase by $\pi/2$, while data "0" decrease the phase by $\pi/2$. The change in carrier frequency from data "0" to data "1", or *vice versa*, is equal to half the bit rate of the incoming data. This is the minimum-frequency spacing which allows the two frequency shift keying (FSK) signals representing symbols "1" and "0" to be coherently orthogonal in that they do not interfere with one another in the process of the detection.

A MSK signal consists of both an in-phase (I) component and a quadrature (Q) component:

$$y_{\rm MSK}(t)=y_{\rm I}(t)+y_{\rm Q}(t).\tag{2}$$

The I component consists of half-cycle cosine pulse defined by

$$y_{\rm I}(t)=\sqrt{\frac{2E_{\rm b}}{T_{\rm b}}}\cos\left(\frac{\pi t}{2T_{\rm b}}\right),\quad -T_{\rm b}\le t\le T_{\rm b};\tag{3}$$

and the quadrature component takes the form

$$y_{\rm Q}(t)=\sqrt{\frac{2E_{\rm b}}{T_{\rm b}}}\sin\left(\frac{\pi t}{2T_{\rm b}}\right),\quad 0\le t\le 2T_{\rm b}.\tag{4}$$

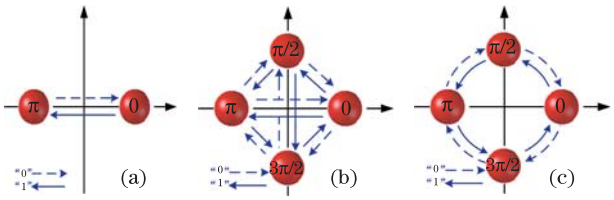

Fig. 1. State diagrams of phase shift for (a) 2PSK, (b) QPSK, and (c) CPM (MSK).

From the above equations, during even bit interval, the I component consists of positive cosine waveform for phase of "0", and negative cosine waveform for phase of "π". During odd bit interval, the Q component consists of positive sine waveform for phase of "$\pi/2$", and negative sine waveform for phase of "$-\pi/2$". The transmitted signal is the sum of I and Q components. Figure 1(c) shows the state diagram for CPM (MSK), which is similar to quadrature phase shift keying (QPSK, as shown in Fig. 1(b)). Any of the four states can arise: 0, $\pi/2$, $-\pi/2$, π. By comparing the phase states of 2PSK (as shown in Fig. 1(a)) and QPSK[15−20], we can find that the phase shift of CPM (MSK) is only $\pi/2$ or $-\pi/2$, and that its phase shift is continuous. As we know, the phase difference of this CPM (MSK) signal between two time instants kT_b and $(k+1)T_\mathrm{b}$, $k \in \{0, \pm1, \pm2, \cdots\}$ is either $-\pi/2$ for bit "0" or $+\pi/2$ for bit "1" in the time span $kT_\mathrm{b} \le t \le (k+1)T_\mathrm{b}$. Hence, the CPM (MSK) signal should be demodulated differentially in the receiver, and this DSP in the electrical domain is achieved easily.

The introduction of CPM (MSK) is due to its potential as a novel coding and modulation method for the generation of OOFDM signals. The source bit stream is mapped by independent MSK coding and is then split into sub-channels. The complex signal of baseband OFDM-CPM in the nth symbol interval can be given by

$$\widetilde{S}(t) = \sum_{k=0}^{N-1} M_k(t) \cdot \exp\left(\mathrm{j}\frac{2\pi kt}{NT_\mathrm{b}}\right), \quad 0 < t < NT_\mathrm{b}. \tag{5}$$

We let

$$M_k(t) = \exp[\mathrm{j}\phi(t, \alpha_k)] = \exp\left[\mathrm{j}\left(\varphi_k + \alpha_k \frac{\pi t}{2NT_\mathrm{b}}\right)\right] \tag{6}$$

be the MSK mapped time-varying symbol in the kth sub-carrier. In Eq. (6), φ_k is the phase state of MSK in the kth sub-carrier, and N is the total number of sub-carriers. In the receiver, for convenience, two sub-carriers and the corresponding transmitted complex signals ($d_1(t)$ and $d_2(t)$) are expressed as

$$d_1(t) = \exp\left[\mathrm{j}\left(\varphi_k + \alpha_k \frac{\pi t}{2NT_\mathrm{b}}\right)\right] \cdot \exp\left(\mathrm{j}\frac{2\pi kt}{NT_\mathrm{b}}\right), \tag{7}$$

$$d_2(t) = \exp\left[\mathrm{j}\left(\varphi_l + \alpha_l \frac{\pi t}{2NT_\mathrm{b}}\right)\right] \cdot \exp\left(\mathrm{j}\frac{2\pi lt}{NT_\mathrm{b}}\right). \tag{8}$$

The frequency spacing (FS) between these two channels is

$$\mathrm{FS} = f_1 - f_2 = (k-l)/NT_\mathrm{b}. \tag{9}$$

By using the basic optical quadrature receiver, the received complex signal can be shown as

$$\widetilde{r}(t) = d_1(t) + d_2(t) + n(t), \tag{10}$$

where $n(t)$ is the complex noise. We define $Z_{k,m}$ as the correlation between the received signals on one symbol interval with all possible transmitted alternatives over that symbol interval. Hence, for a sub-channel, we obtain

$$Z_{k,m} = \mathrm{Re}\left\{\int_0^{NT_\mathrm{b}} \widetilde{r}(t) \cdot \exp\left(-\mathrm{j}\frac{2\pi kt}{NT_\mathrm{b}}\right) \cdot \exp\left[-\mathrm{j}\left(\varphi_m + \alpha_m \frac{\pi t}{NT_\mathrm{b}}\right)\right] \mathrm{d}t\right\}, \quad 0 \le m \le 3, \tag{11}$$

where $\varphi_m = m\pi/4$ is the phase state of one of the branches in MSK trellis, with $\alpha_m \in \{\pm1\}$ being the corresponding input bit. As we know, only two phase states will be used in each symbol interval. It can be verified that $d_2(t)$ will be transformed to d_1 sub-channel by eliminating the ICI through replacing Eqs. (7), (8), and (10) into Eq. (11). The above derivation can be general to multi-carriercase case in the same way.

Figure 2 presents the experimental setup for WDM-PON employing OFDM-CPM downstream and on-off keying (OOK) modulated upstream signals. In the optical line terminal (OLT), four continuous-wave (CW) beams are generated by four distribute feedback (DFB) lasers at frequencies of 193.075, 193.1, 193.125, and 193.15 THz. The linewidth of each DFB laser is 1 MHz. Each input data is first serial-parallel transformed and I/Q mapped in the MSK coding part. CPM (MSK) is used to map bit stream data to the OFDM sub-carriers, and there are 256 sub-carriers. Then the OFDM-CPM baseband waveforms produced by the arbitrary waveform generator (Tektronix AWG710) are continuously output at a sample rate of 20 GHz (8-bit digital-to-analog converter, 4-GHz bandwidth). The guard interval is equal to one quarter of the observation period, and a 5% cyclic prefix (CP) is applied. The 2.5-Gb/s OFDM-CPM baseband signals are generated offline by an OFDM transmitter and then up-converted to 10 GHz to realize radio frequency (RF) OFDM-CPM signals by an electrical mixer. The up-converted electrical spectrum is shown in Fig. 3(a). In each OLT transmitter, the generated RF OFDM-CPM signal is used to modulate a $LiNbO_3$ Mach-Zehnder modulator (MZM). The generated four optical OFDM-CPM signals are multiplexed by an array waveguide grating (AWG), and the optical bandwidth of the AWG is set to the channel spacing (25 GHz). The waveforms of optical OFDM-CPM signal before and after 25-km SMF-28 fiber transmission for a channel downlink in the WDM-PON are measured using Tektronix TDS6604 digital storage oscillscope, as shown in Figs. 3(b) and (c), respectively. It is clearly seen that the amplitude of the measured waveform is lower after transmission due to the existence of fiber loss. We apply commonly used fiber parameters for our experiment: fiber chromatic dispersion of 16 ps/(nm·km), 0.2-dB/km loss, and a nonlinear coefficient of 2.6×10^{-20} m^2/W. After 25-km SMF-28 transmission, the downstream traffic is de-multiplexed by an AWG,

and then the de-multiplexed optical signal is split by a 3-dB optical coupler in each ONU. The ONU has two parts, the receiver part and the signal remodulation part. In the receiver part, the optical OFDM-CPM signal is pre-amplified by a regular erbium-doped fiber amplifier (EDFA), then directly detected through a PIN photodiode with a 3-dB bandwidth of 20 GHz, and sampled by a Tektronix real-time oscilloscope (TDS6154C) at 40 Gsample/s, with all subsequent DSP done off-line. The down-converted 2.5-Gb/s OFDM-CPM signal is detected by a BER tester. The CPM (MSK) signal is a special binary signal, and its detection and demodulation could be achieved easily in electronic domain. The detection of the CPM (MSK) signal requires memory, but its DSP in an off-line way in the transmitter and the receiver is simpler than that of the QPSK signal since the phase shift of CPM (MSK) is only $-\pi/2$ or $+\pi/2$ and its phase shift is continuous. Hence, the memory requirements of the detection of CPM (MSK) signal will not increase the burden of the OFDM detection and demodulation. In the signal remodulation part, each optical OFDM-CPM signal is first filtered by a tunable optical filter with the bandwidth of 0.2 nm, and then it is re-modulated to OOK by an intensity modulator at 2.5 Gb/s with pseudo-random bit sequence (PRBS) of length 2^{31}–1 and multiplexed by an AWG. After the upstream transmission and de-multiplexing by an AWG, each re-modulated signal is detected by a commercial avalanche photodiode (APD) receiver with 2-GHz bandwidth.

Figure 4 shows the received optical spectra diagrams of OFDM-CPM for four CW channels before and after 25-km downstream transmission, and the received optical spectra diagrams of OOK remodulation for four CW channels before and after 25-km upstream transmission. The optical spectra have 0.01-nm resolution of OFDM-CPM (bandwidth at 3 dB is 2.5 GHz), and the FS between each two neighboring carriers is 25 GHz. It is clearly seen that the used scheme precisely achieves frequency domain coexistence of the uplink signal and downlink signal traffic.

We measured the BER performance of OFDM-CPM downstream signal and the measured BER curves for channel 2 (the frequency is 193.1 THz) before and after the 25-km SMF-28 are shown in Fig. 5(a). Moreover, the transmission characteristics and the corresponding constellations of the downstream OFDM-CPM signal are also exhibited in Fig. 5(a). It is found that the receiver sensitivity is improved if OFDM-CPM is selected as the downlink transmitted signal. At a BER of 10^{-3}, the power penalty of 0.1 dB is mainly caused by the degradation of the optical signal-to-noise ratio of the OFDM-CPM signal. Furthermore, with the smaller value of the received power, the less influence is shown for an OFDM-CPM transmission. From the corresponding constellation, the optical OFDM system with MSK

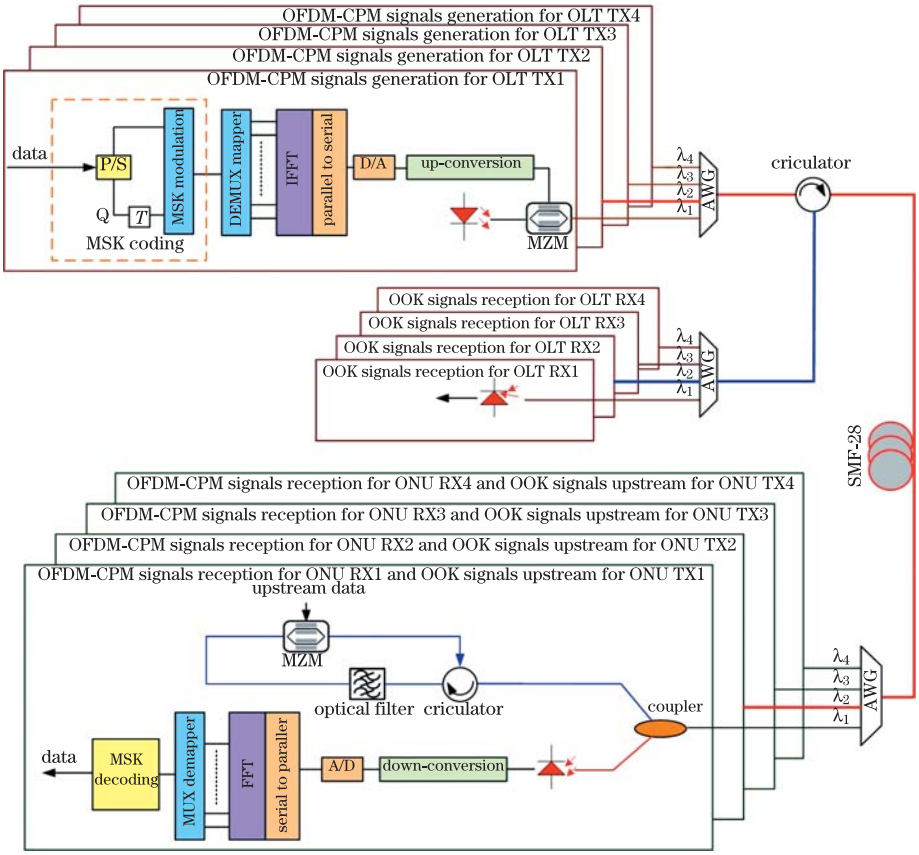

Fig. 2. Schematic diagram for the used bidirectional WDM-PON system. PS: parallel-serial transformation; D/A, A/D: digital-analog conversion; FFT, IFFT: (inverse) fast Fourier transformation; RX: receiver; TX: transmitter; MUX: multiplexing; DEMUX: demultiplexing.

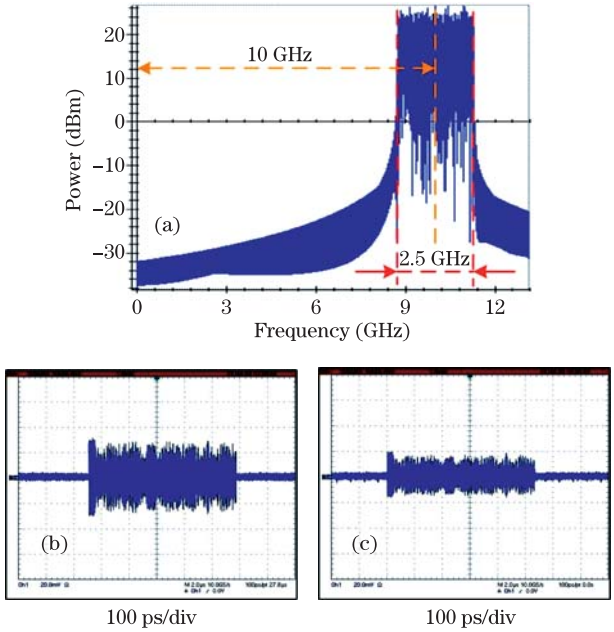

Fig. 3. (a) Up-converted electrical spectrum, measured waveforms of (b) optical OFDM-CPM signal before and (c) after 25-km SMF-28 transmission for a channel downlink in the WDM-PON.

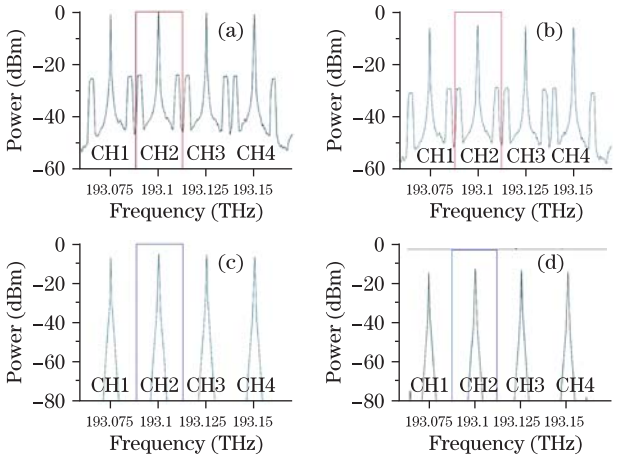

Fig. 4. Received optical spectra diagrams of OFDM-CPM for 4 CW channels (a) before and (b) after downstream 25-km transmission; received optical spectra diagrams of OOK remodulation for 4 CW channels (c) before and (d) after upstream 25-km transmission.

coding and decoding has the property of phase continuity. This feature will reduce the complexity of receiver design, because each phase shift is constant $\pi/2$ when the transfer of signal constellation points occurs. Figure 5(b) illustrates the measured BER curves of channel 2 and the corresponding eye diagram for upstream signals after transmission. It can be clearly seen that the eye diagram is widely opened after transmission. The power penalty is less than 0.4 dB after transmission over 50-km SMF-28 (25-km downstream+25-km upstream) at a BER of 10^{-9}. The power penalty is caused mainly by the accumulated dispersion at the 50-km SMF-28 fiber and the signal re-modulation process at the ONU part.

In conclusion, we have proposed and experimentally

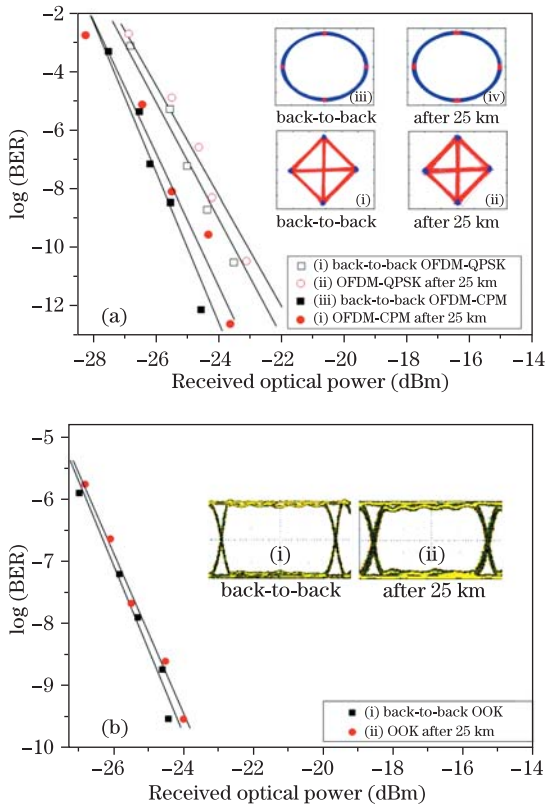

Fig. 5. (a) BER curves at back-to-back and after 25-km SMF-28, and the corresponding constellations for OFDM-CPM and OFDM-QPSK signals; (b) BER curves and the corresponding eye diagrams before and after 25-km SMF-28 for upstream signals.

demonstrated a novel method to generate an OFDM-CPM signal in a WDM-PON as the downlink signal. For OFDM-CPM signals, slighter downstream transmission impairments are introduced in comparison with OFDM-QPSK signals when the signals pass through 25-km SMF-28 fiber. This scheme could be used for optical signal simultaneous uplink by sharing the same optical components such as the optical circulators. The separated optical carrier can be reused for uplink data modulation, hence the ONU can be further simplified and the cost is reduced. We evaluate the BER performance. The power penalty for the downlink data after transmission over 25-km SMF-28 fiber is 0.1 dB, while for the uplink data, the power penalty after transmission over 50-km SMF-28 fiber is less than 0.4 dB. Because MSK is a special type of binary continuous phase-frequency shift keying, it can simplify DSP. And the proposed scheme employs optical OFDM-CPM signal as the downlink signal, which has much better BER performance than OFDM-QPSK. It is a competitive scheme in the future access network.

This work was partially supported by the National "973" Program of China (No. 2010CB328300), the National Natural Science Foundation of China (Nos. 600837004 and 60777010), the National "863" Program of China (Nos. 2009AA01Z253 and 2009AA01A347), the Chinese Postdoctoral Science Foundation (No. 20090460593), the Shanghai Postdoctoral Science Foundation (No. 10R21411600), the Open Fund of Beijing University of Posts and Telecommunications, and the Shuguang Fund.

References

1. J. Armstrong, J. Lightwave Technol. **27,** 189 (2009).
2. W. Shieh, H. Bao, and Y. Tang, Opt. Express **16,** 841 (2008).
3. A. Lowery, L. Du, and J. Armstrong, in *Proceedings of OFC 2006* PDP39 (2006).
4. J. Yu, Z. Jia, and G.-K. Chang, and X.-J. Xin, in *Proceedings of ECOC 2009* 6.5.2 (2009).
5. J. Yu, M.-F. Huang, D. Qian, L. Chen, and G.-K. Chang, IEEE Photon. Technol. Lett. **20,** 1545 (2008).
6. J. Yu, Z. Jia, P. N. Ji, and T. Wang, in *Proceedings of OFC 2007* OTuH8 (2007).
7. J. M. Tang, P. M. Lane, and K. A. Shore, IEEE Photon. Technol. Lett. **18,** 205 (2006).
8. A. J. Lowery and J. Armstrong, Opt. Express **13,** 10003 (2005).
9. X. Liu and F. Buchali, Opt. Express **16,** 21944 (2008).
10. C. W. Chow, C. H. Yeh, and C. H. Wang, IEEE Photon. Technol. Lett. **21,** 715 (2009).
11. J. Yu, M.-F. Huang, D. Qian, W. Wei, T. Wang, and G.-K. Chang, IEEE Photon. Technol. Lett. **21,** 1259 (2009).
12. C.-H. Yeh, C.-W. Chow, and C.-H. Hsu, IEEE Photon. Technol. Lett. **22,** 118 (2010).
13. J. Mo, Y. Dong, Y. Wen, S. Takahashi, Y. Wang, and C. Lu, in *Proceedings of ECOC 2005* Thl.2.3 (2005).
14. L. Couch, *Digital and Analog Communication Systems* (in Chinese) X. Luo, P. Ren, C. Tian, (trans.) (Publishing House of Electronics Industry, Beijing, 2002).
15. Y. Shao, S. Wen, L. Chen, and J. Yu, Chinese J. Lasers (in Chinese) **35,** 1201 (2008).
16. Y. Shao, J. Li, L. Cheng, Y. Pi, S. Wen, and L. Chen, Chinese J. Lasers (in Chinese) **35,** 574 (2008).
17. Y. Shao, N. Chi, C. Hou, W. Fang, J. Zhang, B. Huang, X. Li, S. Zou, X. Liu, X. Zheng, N. Zhang, Y. Fang, J. Zhu, L. Tao, and D. Huang, J. Lightwave Technol. **28,** 1770 (2010).
18. Y. Shao, S. Wen, L. Chen, Y. Li, and H. Xu, Opt. Express **16,** 12937 (2008).
19. Y. Shao, L. Chen, S. Wen, Y. Xiao, L. Cheng, H. Xu, and Y. Pi, Opt. Commun. **281,** 3658 (2008).
20. Y. Shao, L. Chen, and S. Wen, Microw. Opt. Technol. Lett. **49,** 755 (2007).